# Optimal Cuts of Langasite, $La_3Ga_5SiO_{14}$ for SAW Devices

Natalya Naumenko, *Member, IEEE*, and Leland Solie, *Fellow, IEEE*

***Abstract*—The results of a theoretical and experimental investigation of the SAW propagation characteristics in an optimal region of langasite defined by the Euler angles $\varphi$ from $-15°$ to $+10°$, $\theta$ from $120°$ to $165°$, and $\psi$ from $20°$ to $45°$ are presented. Based on temperature coefficients of the elastic constants derived from experimental data, some optimal orientations of langasite characterized by high electromechanical coupling factor ($k^2$), zero power flow angle (PFA) and low or zero temperature coefficient of frequency (TCF) were found. The SAW velocity in the region of interest is highly anisotropic; this results in a significant amount of diffraction, which must be taken into account in the search for orientations useful for SAW devices. An orientation having simultaneously zero PFA, zero TCF, negligible diffraction, and relatively high piezoelectric coupling has been found and verified experimentally. The experimental results are in excellent agreement with the calculated SAW characteristics. The frequency response of a SAW device fabricated on the optimal cut of langasite is presented and demonstrates that high performance SAW filters can be realized on this optimal cut of langasite.**

## I. Introduction

Recent progress in the development of communication systems has given rise to the further development of SAW devices, which are often utilized as the key elements in such systems. The performance specifications required of the SAW IF filters cannot always be realized if only the three customary crystalline materials are implemented as substrates, i.e., quartz, lithium niobate, and lithium tantalate. Therefore, there is a strong need for new piezoelectric materials that can enhance the performance capabilities of SAW devices. To provide low insertion loss, a new substrate material is expected to exhibit strong or moderately strong piezoelectric coupling. A new substrate also must provide minimal change of frequency with a corresponding change in temperature. At the same time, SAW propagation on this new substrate must have minimal power flow angle and minimal diffraction. It also is desirable that the substrate demonstrate sufficiently low acoustic propagation loss in the IF frequency range. It is not difficult to find substrates that provide any of these desirable properties, but it is not possible to satisfy all of these requirements in a single orientation of any of the three commonly used materials. The challenge is to find a new material that has an orientation or range of orientations which will simultaneously satisfy all of these requirements.

In addition to these technical requirements, a new material must have the potential to be commercially available at a reasonable price, which means that the growth technique can not be very complicated or expensive. It must be possible to grow large-size crystals with a diameter of 3 or 4 inches. For IF filters, especially designed for commercial applications, a low SAW velocity is preferred in order to minimize the chip and package size, and consequently reduce the cost of the SAW device.

At present the only material capable of satisfying all of the technical requirements is lanthanum gallium silicate, $La_3Ga_5SiO_{14}$, or langasite This crystal was synthesized in Russia in the early 1980s [1] and soon proved to be a moderately strong piezoelectric with an electromechanical coupling factor a few times higher than that of quartz. For most IF bandwidths, the increase in coupling of langasite is sufficient to enable a significant reduction in insertion loss in comparison to quartz. Being isomorphous to quartz (point symmetry class *32*), langasite "inherited" the specific temperature behavior of quartz, including the existence of temperature-compensated orientations for bulk and surface acoustic waves.

Langasite can be grown from melt by the well developed Czochralski method, and large size crystals of good quality have been successfully grown [2], [3]. The propagation loss measured in langasite at gigahertz frequencies is lower than that in quartz [4], which makes langasite attractive for high-frequency devices. The absence of phase transitions up to the melting point $T_0 = 1470°C$ opens the possibility of high-temperature applications. Compared to lithium niobate or lithium tantalate, langasite has an advantage of having a more stable chemical composition, due to a narrower region of homogeneity. Therefore, one can expect minimal variations in the SAW characteristics between as-grown crystals, though the same feature brings some difficulty into the growth process. Another advantage of langasite compared to customary SAW materials is the SAW velocity, which is lower than that of quartz by 15–30%.

The successful combination of these properties makes langasite a promising new material for future SAW devices, provided that all these advantages are combined in at least one orientation. A numerical analysis of the SAW characteristics in singly rotated cuts of langasite has revealed that none of these orientations exhibits simultaneously high piezoelectric coupling, low temperature coefficient of frequency (TCF), small power flow angle (PFA),

and minimal diffraction. However, because no orientation either singly or doubly rotated on any other SAW substrate satisfies these conditions, it is necessary to extend the search further. A thorough numerical investigation of SAW propagation characteristics in doubly rotated cuts has shown that there is a wide crystallographic area in which some optimal combinations of SAW properties can be obtained. This area was first defined in [5] by the following intervals of the Euler angles: $\varphi$ from $-15°$ to $+10°$, $\theta$ from $120°$ to $165°$, $\psi$ from $20°$ to $45°$, and with zero $\varphi$ the best combination of SAW characteristics was found to exist in langasite when $\theta$ changes from $125°$ to $145°$, and $\psi$ from $14°$to $34°$ [6]. The optimal area includes the absolute maximum of electromechanical coupling factor $k^2$ for langasite (about 0.5%), and in a number of orientations moderately high coupling is combined with low or zero TCF and PFA values. The conclusion that this angular region is characterized by an excellent combination of SAW characteristics was recently confirmed by several groups of researchers, both theoretically and experimentally [7]–[11]. Experimental SAW characteristics have been reported for some promising orientations belonging to the optimal area, such as: (0°, 140°, 22.5°) [7], (0°, 142°, 24.5°) [9], (0°, 140°, 24°) [10], and (0°, 140°, 25°) [11]. These and other orientations exhibit good temperature stability, low power flow angle, and moderately high piezoelectric coupling ($0.3 < k^2 < 0.4\%$). It was also found [6], [10] that the anisotropy parameter $\gamma$, which determines SAW diffraction, is near the optimal value $\gamma = -1$ in some orientations. This paper presents the results of further numerical and experimental investigation of the SAW propagating in the optimal area of langasite. The main purpose of this investigation was to find the orientation that combines the maximum number of optimal SAW characteristics.

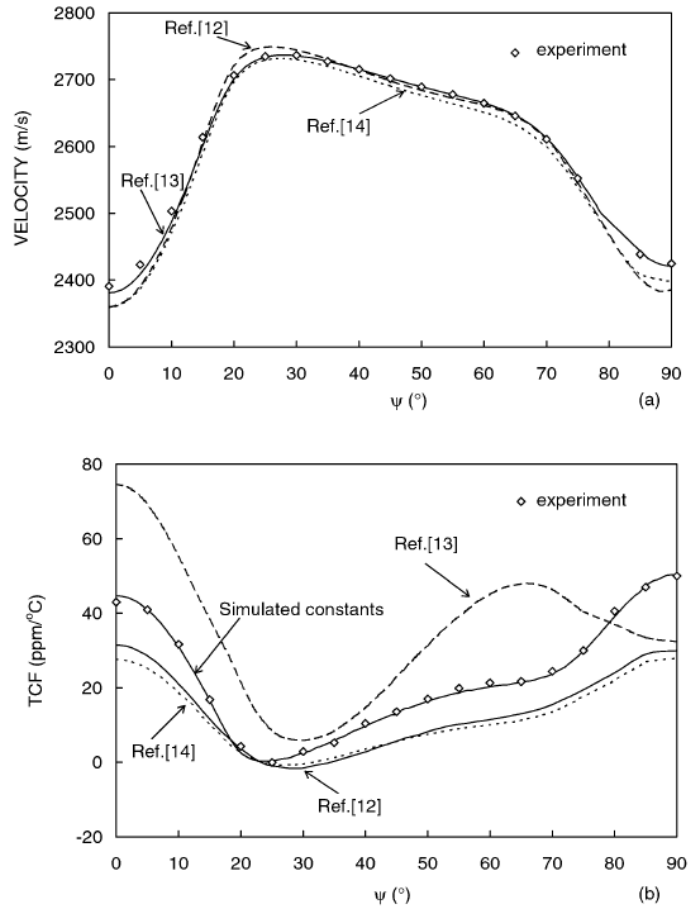


Fig. 1. Calculated and experimental SAW velocities (a) and temperature coefficients of frequency (b) as functions of angle $\psi$ in orientations of langasite with Euler angles (0°, 136.5°, $\psi$). The calculations are based on material constants from [12]–[14] and temperature coefficients of elastic constants from Table I.

## II. Investigation of SAW Propagation in the Optimal Area

A theoretical investigation of SAW characteristics must be based on reliable material data, including the elastic, piezoelectric, and dielectric constants of the crystal and their temperature dependencies. To analyze the effect of material constants on the calculated SAW characteristics, calculations were made with three different sets of langasite constants [12]–[14]. For orientations of the optimal area, SAW velocities changed by 1–2% when different material constants were used. These values agree with the common accuracy of material constant measurements. As a result, the power flow angle vanishes nearly in the same orientations for any constants. The TCF and the electromechanical coupling factor are more sensitive to the choice of material data. For example, the absolute maximum of the coupling factor changes from $k^2_{max} = 0.46\%$ to $k^2_{max} = 0.55\%$ if the material constants from [12] are replaced by the constants from [13].

While selecting suitable material data for a theoretical investigation of the SAW behavior in the optimal area, we focused on obtaining accurate values of PFA, anisotropy parameter, and TCF. The first two characteristics were dependent on the anisotropy of the SAW phase velocity. In Fig. 1(a) the calculated and measured velocities are presented for SAW propagation in the Y+46.5° cut of langasite with Euler angles 0°, 136.5°, $\psi$. Calculations were based on three different sets of material constants [12]–[14]. The SAW phase velocities were derived using a pair of unweighted narrowband transducers ($\lambda$ equal to 16 $\mu$m, where $\lambda$ is the SAW wavelength) and measuring the center frequency of the passband. The thickness of the aluminum electrodes was negligible ($h/\lambda = 0.002$). Fig. 1(a) demonstrates that, at least within the angular range considered by these curves, the best agreement between calculated and measured SAW velocities is achieved when the material constants from [13] are used. This conclusion agrees with the results obtained by other researchers [9]. Therefore, further calculations of SAW characteristics in the optimal area are based on the material constants from [13].

A comparison of the experimental and calculated temperature characteristics of SAW propagation in the Y+46.5° cut of langasite [Fig. 1(b)] revealed that none of the reported sets of temperature coefficients of the ma-

terial constants [12]–[14] describes the temperature dependence of frequency adequately, though all sets predict the existence of orientations with zero TCF in the optimal area. Therefore, improved temperature coefficients of the elastic constants were derived from the experimental dependence of TCF($\psi$) in the Y+46.5° cut, $Tc_{11} = -53$ ppm/°C, $Tc_{12} = -85$ ppm/°C, $Tc_{13} = -100$ ppm/°C, $Tc_{14} = -310$ ppm/°C, $Tc_{33} = -94$ ppm/°C, $Tc_{44} = -55$ ppm/°C [15].

Though accurate simulation of material constants require measurement of TCF in at least three mutually orthogonal crystal planes, the temperature coefficients from experimental data for the Y+46.5 plane provide excellent agreement between theoretical and experiment temperature behavior of the SAW in this cut [Fig. 1(b)] and in a wide area around it. The calculation of TCF in the same cut using other reported sets of temperature coefficients simulated from experimental data [7], [10], [16] has shown that all these sets provide good agreement with our experimental data in the interval of propagation angles $\psi$ from 15° to 35°. Outside this interval the difference between calculated and experimental TCF values increases. This difference is greatest for the temperature coefficients reported in [7] and does not exceed 4 ppm/°C for the coefficients simulated in [10]. For our simulated temperature coefficients, the difference between the numerical and experimental TCF values is smaller than 1.5 ppm/°C within the whole interval of propagation angles from 0° to 90° in the Y+46.5° cut.

The calculated characteristics of SAW propagation in some rotated Y-cuts of langasite, defined by the Euler angles (0°, 135° − 150°, $\psi$), are plotted in Fig. 2(a)–(e) as functions of the propagation angle $\psi$. In addition to the phase velocity V on a free surface, power flow angle $\phi$, electromechanical coupling factor $k^2$, and TCF, the calculation of the anisotropy parameter $\gamma = \partial\phi/\partial\psi$ has been performed. One can see that, for any angle $\theta$ in the interval $\theta$ from 135° to 150°, the PFA($\psi$) dependence crosses the zero line when $\psi$ changes from 24° to 30°. If $\theta$ is between 135° and 140°, the TCF values do not exceed 4 ppm/°C in the same interval of $\psi$. For example, in the orientation (0°, 140°, 25.5°), TCF<1 ppm/°C, PFA=0, V=2747 m/s, and $k^2 = 0.37\%$. The electromechanical coupling factor is maximum ($k^2 = 0.52\%$) in the orientations (0°, 145° − 150°, 24° − 24.5°). However, these orientations must be implemented with care because of the strong anisotropy in the propagation velocity. Even a small misalignment of 1° from the desired crystal orientation can result in dramatic beam steering, up to 10°. Also, a strong diffraction effect is expected in these orientations, which can cause degradation of the device performance and an increase in the insertion loss. The anisotropy parameter is extremely high around the orientation (0°, 150°, 22.5°) in which $|1 + \gamma| \approx 12$. In this orientation the SAW velocity (2758 m/s) is very close to that of the shear bulk wave (2766 m/s) and coupling of the SAW with a parasitic bulk wave can occur.

However, due to the strong anisotropy in the region of interest, some cuts with $\gamma = -1$ can be found in which full autocollimation of the acoustic beam is expected. For example, in orientations with Euler angles (0°, 135° − 140°, 26° − 27°), in addition to a small PFA (<3°) and low TCF (<2 ppm/°C), nearly zero diffraction can be predicted.

Consider the effect of variations in the first Euler angle on the SAW characteristics in the region of interest. Fig. 3(a)–(e) shows SAW characteristics as functions of the angle $\psi$, and $\varphi$ is fixed within the interval $\gamma$ from −10° to +5° and $\theta = 140°$. Increasing values of V($\psi$) and $k^2(\psi)$ and decreasing values of PFA($\psi$) and TCF($\psi$) are obtained for increasing propagation angles $\psi$ with increasing $\varphi$. Due to this parallel shift of different SAW characteristics, low PFA is combined with a sufficiently high coupling factor $k^2$ and a low TCF in a number of orientations. For example, in the orientation (−10°, 140°, 14°), the SAW is characterized by V=2680 m/s, $k^2$ =0.47%, PFA=0, $\gamma = -2.22$, and TCF=9 ppm/°C. In the orientation (5°, 140°, 31.3°), the SAW propagates with the following characteristics: V=2777 m/s, $k^2$=0.31%, PFA=0.6°, $\gamma = -1$, and TCF= −2 ppm/°C. The electromechanical coupling factor reaches the highest value $k^2$=0.55% in the orientation (−10°, 145°, 12°), this value being the absolute maximum of the coupling factor in langasite. The other SAW properties, V=2687 m/s, PFA=7.5°, $\gamma = -6.7$, and TCF=12 ppm/°C, do not look very attractive.

Fig. 2 and Fig. 3 demonstrate that the choice of a specific orientation in the optimal area depends on the relative priorities placed upon the various SAW propagation characteristics that we desire to optimize. If maximum electromechanical coupling factor is of major importance, langasite orientations with Euler angles (5°, 150°, 29°) with $k^2$=0.50%, or (0°, 150°, 24°) with $k^2$=0.51% can be used. The latter orientation was studied experimentally in [9], and the high value of electromechanical coupling factor was confirmed. In both substrates the TCF is small (7 ppm/°C and 3 ppm/°C), but device performance can suffer from the strong diffraction.

Calculated SAW characteristics for some orientations with zero PFA and various electromechanical coupling factors are presented in Table I. The main drawback of using langasite orientations with coupling factors $k^2$=0.47 − 0.54% is strong diffraction. In orientations with low diffraction, the coupling factors are not as high.

## III. An Optimal Cut of Langasite with Zero PFA, Zero TCF, and Zero Diffraction

If none of the three Euler angles is fixed, it is possible to find an orientation in 3-dimensional space $(\varphi, \theta, \psi)$ in which the SAW is characterized simultaneously by TCF=0, PFA=0, and $\gamma = -1$. Indeed, each of these SAW properties becomes optimal if the corresponding orientation belongs to the characteristic surface in 3-D space. Any characteristic surface (e.g., one defined by PFA=0) can be described in coordinates $(\varphi, \theta, \psi)$ as $\varphi(\theta, \psi)$. Two requirements (e.g., PFA=0 and $\gamma = -1$) can be satisfied simultaneously with a curve in 3-D space, which can be found

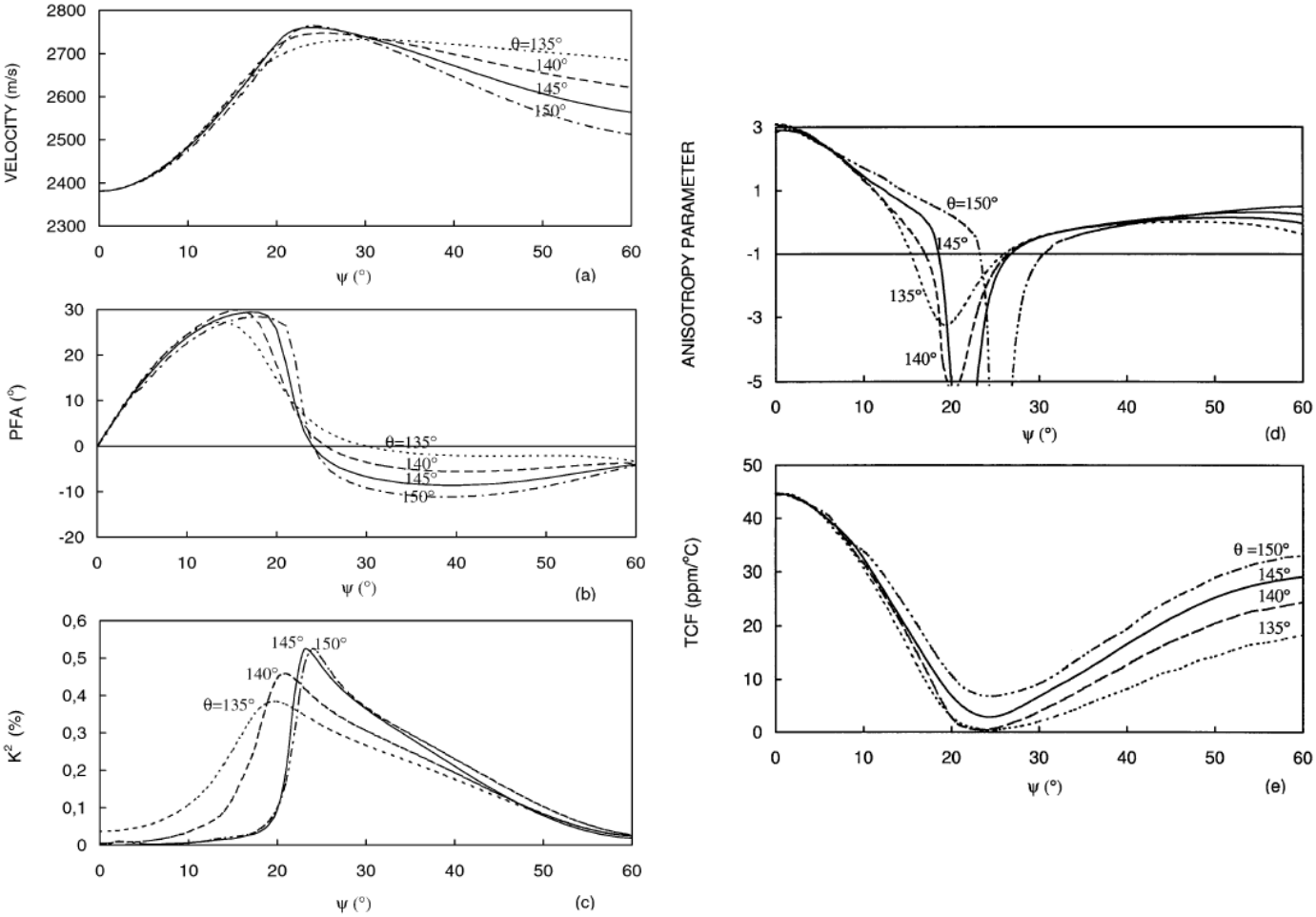


Fig. 2. Calculated characteristics of SAW propagating in orientations of langasite with Euler angles (0°, $\theta$, $\psi$) as functions of angle $\psi$: phase velocity (a), power flow angle (b), electromechanical coupling factor (c), anisotropy parameter (d), and temperature coefficient of frequency (e).

TABLE I
CALCULATED SAW CHARACTERISTICS IN SOME ORIENTATIONS OF LANGASITE

| Euler angles | Velocity (m/s) | $k^2$ (%) | PFA (deg.) | TCF (ppm/°C) | $\gamma = \partial\phi/\partial\psi$ |
|---|---|---|---|---|---|
| (0°, 150°, 24°) | 2765 | 0.51 | 0 | 7 | −4.9 |
| (5°, 150°, 29°) | 2798 | 0.50 | 0 | 3 | −5.5 |
| (10°, 150°, 34°) | 2829 | 0.47 | 0 | −1 | −5.9 |
| (5°, 145°, 29°) | 2793 | 0.42 | 0 | −2 | −2.3 |
| (0°, 140°, 25.5°) | 2747 | 0.37 | 0 | 1 | −1.2 |
| (0°, 138.5°, 26.3°) | 2743 | 0.34 | 0 | 1 | −1.0 |

as the intersection of the corresponding characteristic surfaces. Obviously, a point where this line intersects the third characteristic surface, TCF=0, can exist. In Fig. 4(a) the line of orientations $(\varphi, \theta, \psi)$, characterized by PFA=0 and $\gamma = -1$, is presented by its projections $\theta(\varphi)$ and $\psi(\varphi)$ onto the coordinate planes. The corresponding SAW velocity, $k^2$ and TCF, are illustrated in Fig. 4(b) and (c) as functions of $\varphi$. The temperature behavior of the SAW has been analyzed for two cases: when the surface is free and when it is covered by an aluminum overlay with a thickness $h/\lambda$=0.01. On the free surface, TCF=0 occurs in the orientation (1.8°, 139°, 28°). On the metallized surface with $h/\lambda$=0.01, the calculated optimal cut characterized by PFA=0, $\gamma = -1$ and TCF=0 is defined by the Euler angles (−0.5°, 138°, 26.5°).

To verify these calculations, an experimental investigation of the SAW propagation characteristics was performed in six different wafer cuts around the calculated optimal cut. These cuts are (−1.8°, 134.4°, $\psi$); (0°, 135.6°, $\psi$); (1.8°, 135.6, $\psi$); (1.8°, 137.6°, $\psi$); (−1.8°, 137.6°, $\psi$); and

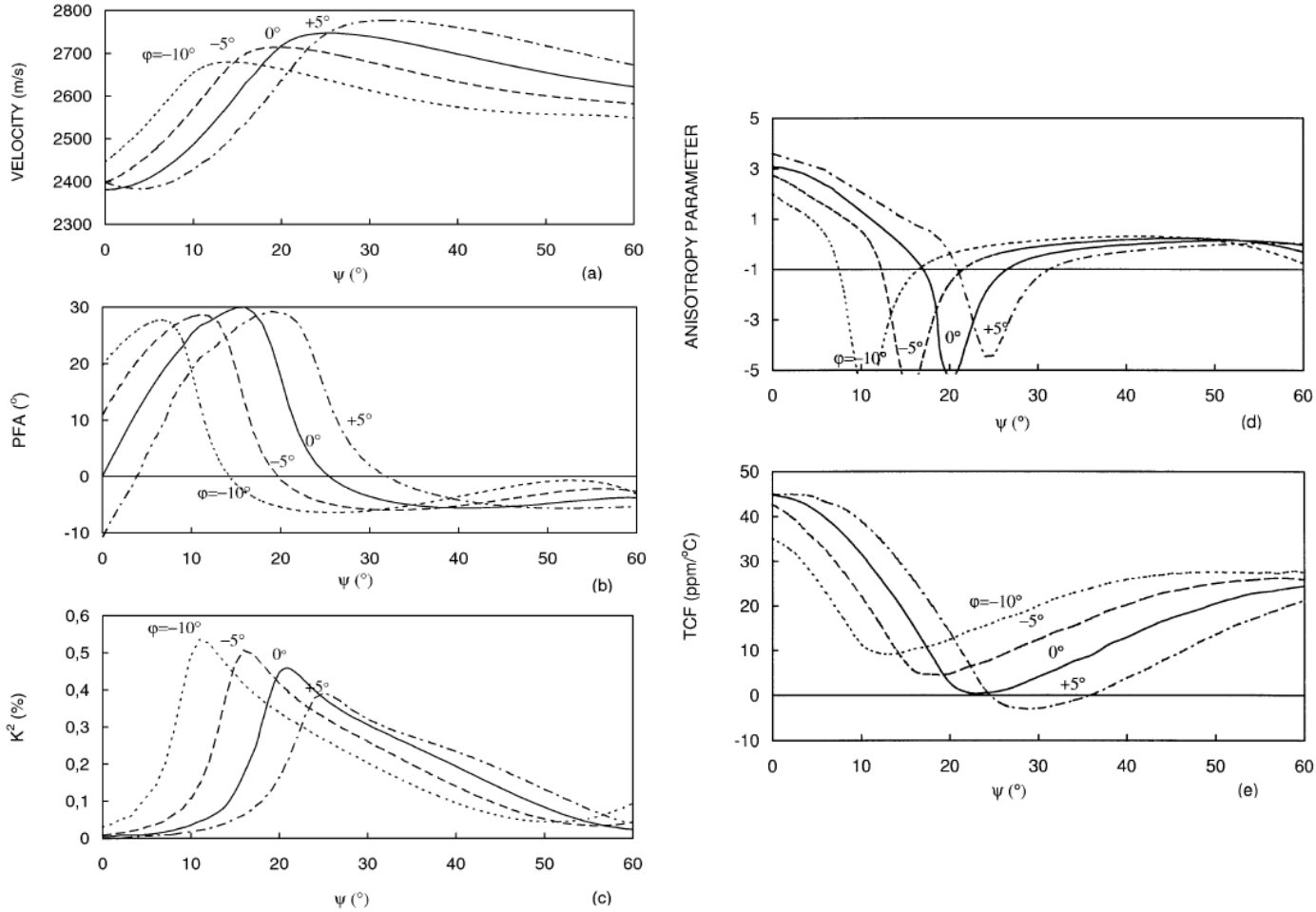


Fig. 3. Calculated characteristics of SAW propagating in orientations of langasite with Euler angles ($\varphi$, 140°, $\psi$) as functions of angle $\psi$: phase velocity (a), power flow angle (b), electromechanical coupling factor (c), anisotropy parameter (d), and temperature coefficient of frequency (e).

($-3.8°$, 135.6°, $\psi$), where $14° < \psi < 34°$. For each cut, the SAW velocity, TCF, PFA, and anisotropy factor were measured or derived from data. Using an interpolation technique, two orientations were found in which PFA=0 and $\gamma = -1$ were expected to occur simultaneously, ($-1.8°$, 137.5°, 25.5°) and (1.8°, 139.6°, 28°). These orientations are shown in Fig. 4. The corresponding points nearly lie on the calculated lines $\theta(\varphi)$ and $\psi(\varphi)$, which proves that there is good agreement between the numerical and experimental results and enables one to predict with high accuracy the optimal cut combining PFA=0, $\gamma = -1$, and TCF=0. Taking into account the TCF values derived from experimental data in these two orientations, 3 ppm/°C and $-1.5$ ppm/°C, respectively [Fig. 4(c)], the optimal cut was determined as (0.5°, 139°, 27°) when the aluminum thickness was negligible. With a very minor compromise in performance, the first Euler angle can be set to zero. This simplifies the cutting of wafers as well as reduces the potential for errors in wafer production. If $\varphi = 0$, the optimal combination of properties PFA=0, $\gamma = -1$, TCF<1 ppm/°C is expected for SAW propagation in the orientation (0°, 138.5°, 26.8°).

In Fig. 5(a) the measured SAW velocities are plotted versus propagation angle $\psi$ in the Y+48.5° rotated cut of langasite with Euler angles (0°, 138.5°, $\psi$); Fig. 5(b) illustrates the power flow angle and anisotropy parameter calculated from the measured velocities V($\psi$). Zero PFA has been obtained at the point $\psi = 26.8°$ with V=2734 m/s, $\gamma = -1.17$, TCF≈0. Zero temperature coefficient of frequency was achieved slightly above room temperature. Measured frequency-temperature characteristics for three propagation angles ($\psi$ =24.8, 26.8, and 28.8°) near the optimal cut are presented in Fig. 6, and the experimentally determined turnover temperature $T_0$ is shown as a function of angle $\psi$ in Fig. 7. In the interval 26.8±3°, the turnover temperature varies between 10°C and 40°C.

Because the SAW velocity is higher in aluminum than in langasite, an aluminum overlay is expected to accelerate surface waves in this material. The calculated effect of a homogeneous aluminum film on the SAW velocity and electromechanical coupling factor $k^2$ are shown in Fig. 8. The coupling factor was estimated as $2(V_f - V_m)/V_f$, where $V_f$ and $V_m$ are the SAW velocities on the "free" and "short" surfaces, respectively. For "free" surface, the change of ve-

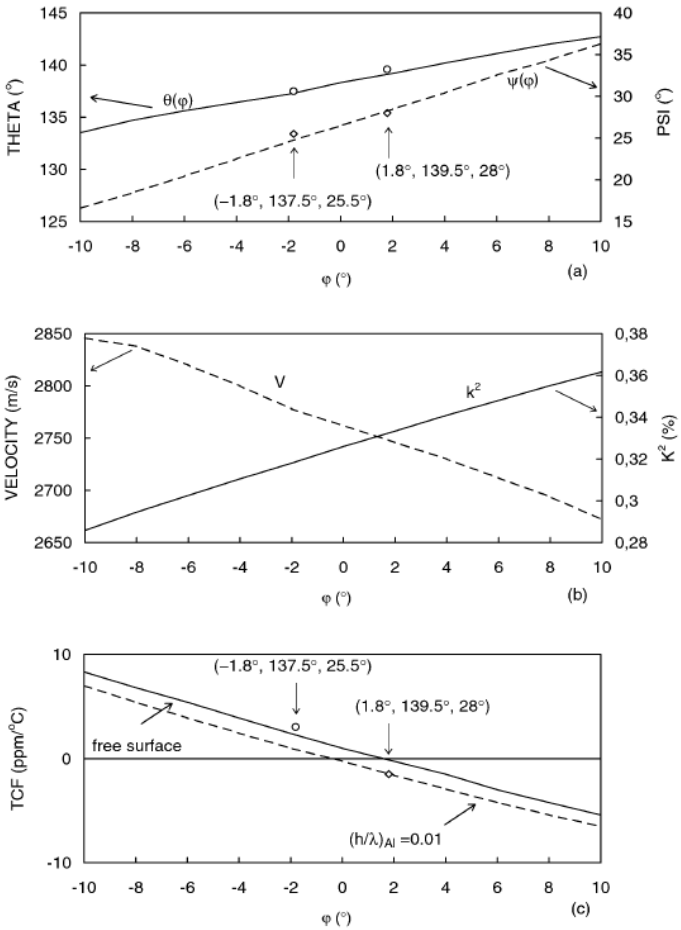


Fig. 4. Calculated orientations of langasite $(\varphi, \theta, \psi)$ characterized by PFA $= 0$ and $\gamma = -1$, plotted as $\theta(\varphi)$ and $\psi(\varphi)$ (a), and SAW characteristics in these orientations: phase velocity (b), TCF on free surface and on metallized surface with aluminum overlay (c). Two experimentally found orientations $(-1.8°, 137.5°, 25.5°)$ and $(1.8°, 139.6°, 28°)$ with PFA $= 0$ and $\gamma = -1$ are indicated by open circles and diamonds, respectively.

locity with thickness was caused by the mechanical loading of the Al layer. Calculations have confirmed the increase in SAW velocity with metal thickness. The coupling factor is expected to grow, and the turnover temperature moves to lower values with increasing Al thickness.

A typical frequency response of a bandpass filter device made on the optimal cut of langasite $(0°, 138.5°, 26.8°)$ is presented in Fig. 9. The bandwidth is 5.0 MHz centered at 190 MHz. The matched insertion loss is 14 dB, and the rejection is 41 dB. It should be pointed out that the sidelobe response on the high side of the passband is not a bulk wave response but rather a phase error associated with the transducer design which is correctable, in which case the rejection should exceed 50 dB. The filter is implemented using tapered SPUDT transducers using SPUDT electrode structures suitable for natural SPUDT substrates. The SPUDT tap structures use four electrodes per wavelength. The tap structures for NSPUDT substrates [8] are completely different for propagation in the forward and reverse directions (as a matter of definition, the positive direction can be chosen to be "substantially" in the direction of the

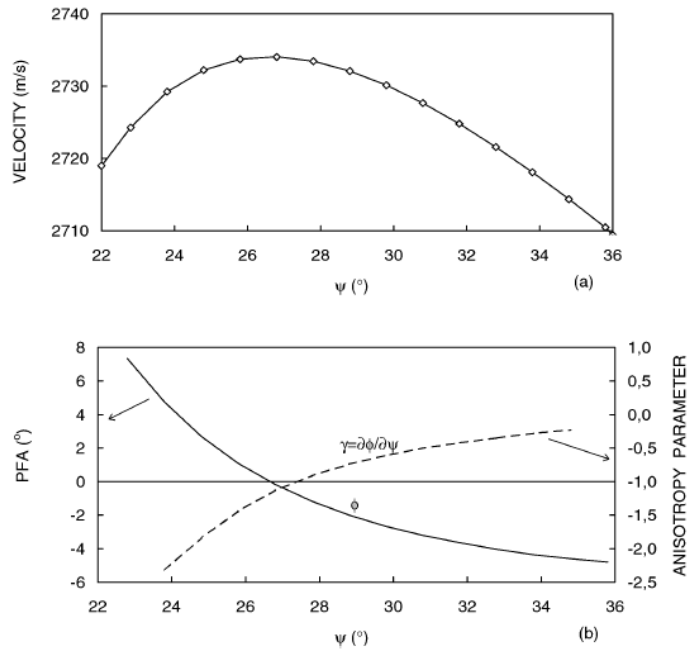


Fig. 5. Experimental SAW velocities (a) and calculated from experimental data power flow angles $\phi$ and anisotropy parameters $\gamma$ (b) as functions of angle $\psi$ in orientations with Euler angles $(0°, 138.5°, \psi)$.

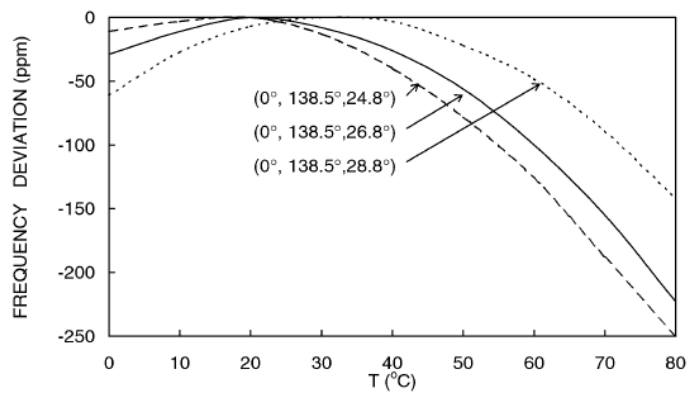


Fig. 6. Frequency deviation versus temperature dependencies measured in three propagation directions on Y+48.5 cut of langasite, Euler angles $(0°, 138.5°, \psi)$.

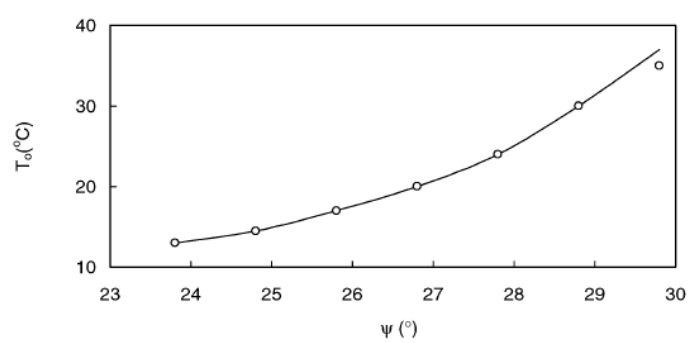


Fig. 7. Measured turnover temperature as function of angle $\psi$ in orientations with Euler angles $(0°, 138.5°, \psi)$.

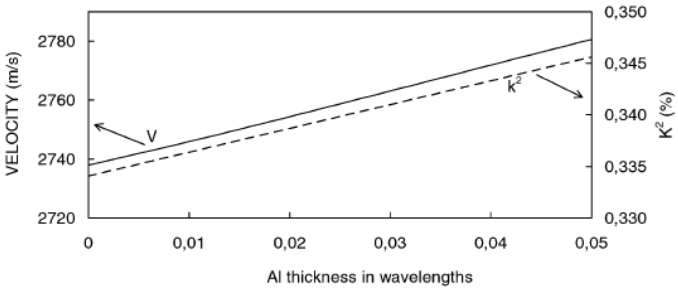


Fig. 8. Calculated SAW velocity and electromechanical coupling factor as functions of normalized thickness of aluminum overlay in (0°, 138.5°, 26.8°) cut of langasite.

+X axis, or more precisely 26.8° away from the +X axis, as $\psi$ =26.8°). The tap structures in the forward direction can be "solid" electrodes (or two electrodes per wavelength), or they can use four electrodes per wavelength, in which case the gap between electrodes of the same polarity is smaller than the gap between electrodes of opposite polarity. The latter choice was used here. Similarly, the tap structures in the reverse direction also use four electrodes per wavelength, but here the gap between electrodes of the same polarity are larger than the gap between electrodes of opposite polarity. The electrodes are rather narrow (i.e., approximately $\lambda/10$) and the acoustic aperture is $95\lambda$, so resistive losses in the electrodes contribute about 8–9 dB to the insertion loss. The triple transit suppression is 55 dB and is evidence that the SPUDT taps are in fact helping to cancel the regeneration-induced triple transit signal. In a filter with an identical design, except for bidirectional taps, the matched triple transit suppression was only 31 dB.

## IV. Conclusions

Theoretical and experimental investigations of the SAW propagation characteristics were performed on orientations of langasite in a range defined by the Euler angles ($-15° - +10°$, $120° - 165°$, $20° - 45°$). Combining the elastic, piezoelectric and dielectric constants of Ilyaev *et al.* [11] with temperature coefficients derived from experimental data provided excellent agreement between calculated and measured SAW characteristics. Orientations of langasite with zero PFA, small TCF, and various values of electromechanical coupling factors $k^2$ ranging from 0.34 to 0.51% were found. Analysis of the anisotropy parameter has revealed that, in orientations with higher coupling factors, stronger SAW diffraction is expected. Orientations in which the SAW is characterized by zero power flow angle and full autocollimation (minimal diffracion) of the acoustic beam ($\gamma = -1$) were calculated and presented as a line in a 3-D space of Euler angles, and the accuracy of these results were proved experimentally. Among these orientations, the cut with TCF=0 was discovered. For a negligible metal overlayer, this cut was defined by the Euler angles (1.8°, 139°, 28°). Measured SAW data that involve a thin aluminum film indicates that the optimal orientation is defined by the angles (0°, 138.5°, 26.8°), where V=2734 m/s, PFA=0, $\gamma = -1.17$, TCF≈0. The frequency response of a SAW filter made on this orientation of langasite is presented.

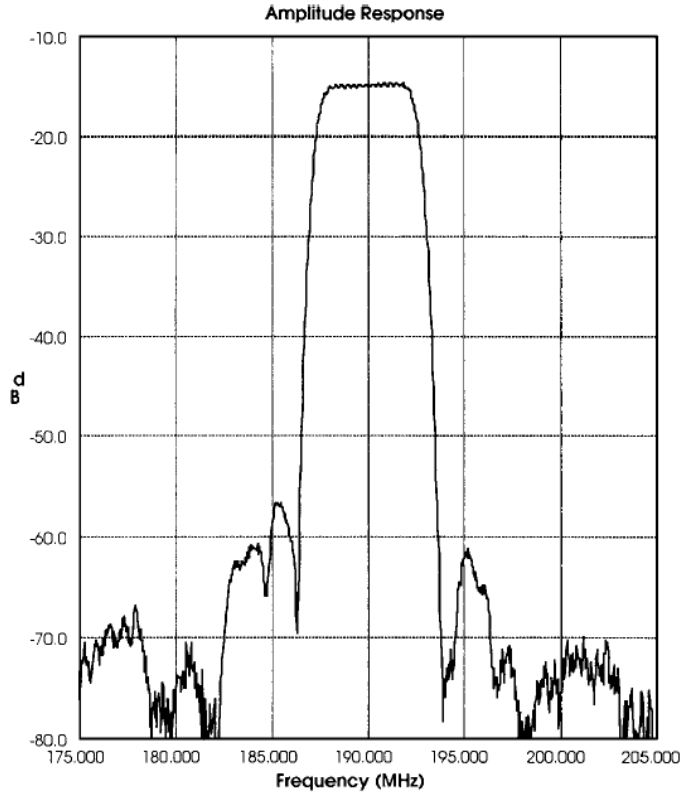


Fig. 9. Frequency response of a SAW filter with tapered SPUDT electrode structures, made on the optimal cut of langasite (0°,138.5°, 26.8°).

## Acknowledgment

The authors thank Saywer Research and Crismatec for supplying the test wafers of langasite.

## References

[1] B. V. Mill, A. V. Butashin, G. G. Khodzhabagyan, E. L. Belokoneva, and N. V. Belov, "Modified gallates with the structure $Ca_3Ga_2Ge_4O_{14}$," *Sov. Phys.–Dokl*, vol. 27, p. 434, 1982.

[2] O. A. Buzanov, A. V. Naumov, U. U. Nechaev, and S. N. Knyazev, "A new approach to the growth of langasite crystals," in *Proc. IEEE Int. Freq. Contr. Symp.*, 1996, pp. 131–136.

[3] B. Chai, J. J. Lefaucheur, Y. Y. Ji, and H. Qiu, "Growth and evaluation of large size LGS ($La_3Ga_5SiO_{14}$), LGN ($La_3Ga_{5.5}Nb_{0.5}O_{14}$) and LGT ($La_3Ga_{5.5}Ta_{0.5}O_{14}$) single crystals," in *Proc. IEEE Int. Freq. Contr. Symp.*, 1998, pp. 748–758.

[4] G. D. Mansfeld, "Measurements of acoustic wave attenuation in $La_3Ga_5SiO_{14}$ using HBAR technique," in *Proc. IEEE Int. Freq. Contr. Symp.*, 1994, pp. 35–39.

[5] N. F. Naumenko and V. S. Orlov, "High frequency SAW device," RU Patent No. 2099857, Dec. 1997, priority Jan. 10, 1996.

[6] N. F. Naumenko and V. S. Orlov, "High frequency SAW devices on langasite," U.S. Patent No. 5,917,265, Jun. 1999, priority Jan. 10, 1996.

[7] K. Inoue and K. Sato, "Propagation characteristics of surface acoustic waves on langasite," *Jap. J. Appl. Phys.*, part 1, vol. 37, pp. 2914–2917, 1998.

[8] M. Takeuchi, M. Tanaka, and Y. Imanishi, "SAW reflection characteristics and NSPUDT orientations of langasite," in *Proc. IEEE Int. Ultrason. Symp.*, 1998, pp. 297–300.

[9] M. Kadota, J. Nakanishi, T. Kitamura, and M. Kumatoriya, "Surface acoustic wave properties on various rotated Y-cut langasite crystal substrates grown by Czochralski method," in *Proc. IEEE Int. Ultrason. Symp.*, 1998, pp. 311–314.

[10] A. Bungo, C. Jian, K. Yamaguchi, Y. Sawada, S. Uda, and Y. Pisarevsky, "Analysis of surface acoustic wave properties of the rotated Y-cut Langasite substrate," *Jpn. J. Appl. Phys.*, part 1, vol. 38, no. 5B, pp. 3239–3243, 1999.

[11] E. H. Briot, E. Bigler, S. Ballandras, G. Marianneau, and M. Solal, "Experimental measurements of velocities and temperature effects for SAW on Y-rotated and X-cuts of langasite," in *Proc. Joint Meeting EFTF-IEEE IFCS*, 1999, pp. 883–886.

[12] A. A. Kaminskii, I. M. Silvestrova, S. A. Sarkisov, and G. A. Denisenko, "Investigation of trigonal $(La_{1-x}Nd_x)Ga_5SiO_{14}$ (II Spectral laser and electromechanical properties)," *Phys. Stat. Sol.(a)*, vol. 80, pp. 607–620, 1983.

[13] A. B. Ilyaev, B. S. Umarov, L. A. Shabanova, and M. F. Dubovic, "Temperature dependence of electromechanical properties of LGS crystals," *Phys. Stat. Sol.(a)*, vol. 98, pp. K109–K114, 1986.

[14] S. Sakharov, P. Senushenkov, A. Medvedev, and Y. Pisarevsky, "New data on temperature stability and acoustic losses of langasite crystals," in *Proc. IEEE Int. Freq. Contr. Symp.*, 1995, pp. 647–652.

[15] N. F. Naumenko and L. Solie, "Optimal cut of langasite for high performance SAW devices," in *Proc. Ultrason. Symp.*, 1999, pp. 243–248.

[16] R. Taziev, "Langasite: What temperature coefficients of material constants are correct?," in *Proc. Joint Meeting EFTF-IEEE IFCS*, 1999, pp. 835–838.